Rearrangements in a two-dimensional packing of disks

M. A. Aguirre,* A. Calvo,† I. Ippolito,‡ A. Medus, and M. Mancuso
Grupo de Medios Porosos, Departamento de Física, Facultad de Ingeniería, Universidad de Buenos Aires, Capital Federal (1063), Argentina

(Received 8 June 2005; revised manuscript received 23 December 2005; published 28 April 2006)

Several aspects of the dynamics of a granular two-dimensional (2D) packing of disks slowly tilted until the system loses stability and an avalanche takes place are discussed. The evolution of the system, constructed with monodisperse disks placed on a thin cell, is studied by image analysis. As in the 3D case (packing of spheres), the system undergoes several rearrangements of different magnitude before the avalanche takes place. For thick systems, not only are small rearrangements detected but also displacements of large clusters of disks are observed in the bulk and on the free surface of the packing. In particular, characteristic angles and the avalanche mass were determined for samples of different heights. On thick systems, velocity fields of large rearrangements are presented and changes in the internal structure of the packing produced by these rearrangements are analyzed. It is found that the main effects of rearrangements is to increase the disorder of the system. Also, as the disorder of the system increases its stability threshold decreases.

DOI: 10.1103/PhysRevE.73.041307 PACS number(s): 45.70.Mg, 45.70.Ht, 05.45.−a

I. INTRODUCTION

Avalanche processes in three-dimensional sphere packings have been exhaustively studied [1,2]. Prior to the avalanche, several rearrangements (movements of spheres) of different sizes (number of spheres in motion) are observed at the free surface; their size distribution and frequency have been thoroughly studied. Indirect evidence that larger rearrangements involve not only the free layer but also the bulk has been found.

In order to verify whether large rearrangements affect the bulk of the system and prepare it for the avalanche, experiments were made with a two-dimensional disordered packing of disks, slowly tilted until it loses its stability. The general characteristics of the dynamics of these large events are studied and modifications of the contact network due to large rearrangements are characterized by image analysis. Special interest will be devoted to the disks velocity profiles during these events.

With respect to contact network changes there have been numerical studies [3] in a two-dimensional granular system similar to the one described in Sec. II. The author found that as the system evolves toward the avalanche, the packing increases its anisotropy.

On the other hand, grain velocity profiles during granular flow have been analyzed experimentally and theoretically in different geometries. Komatsu *et al.* [4] use a quasi two-dimensional system in which the particles form a triangular shaped pile with rapid flow on the free surface and creep motion for deep layers. In these deep layers they found an exponential dependence of the velocity on the distance to the free surface. They also developed a semiempirical model based on void migration which explains the experimental variation.

Bonamy *et al.* [5] investigate steady granular surface flows in a rotating drum. They found a velocity profile decreasing exponentially with depth in the quasistatic phase and remaining linear in the flowing layer.

Veje *et al.* [6] describe experiments on a two-dimensional Couette system in which the inner cylinder rotates and the outer one is at rest. In the shear zone, the azimuthal velocity decreases exponentially with the distance to the moving wall with a small Gaussian correction.

In other experiments, Mueth *et al.* have shown [7] that in a three-dimensional (3D) Couette cell with the inner cylinder rotating filled with seeds or glass spheres the azimuthal velocity can be expressed as a product of an exponential decay and a Gaussian. More precise experiments were later performed by Mueth [8] using the same experimental device with a mixture of stainless steel balls. He found again that variation of the velocity with the distance to the moving wall is well described by the product of an exponential and a Gaussian. The experimental setup and procedure are described in Sec. II. In Sec. III the onset of the avalanche is studied as a function of the packing height. In Sec. IV we analyze in detail large rearrangements occurring in the bulk of thick systems including about 20 layers, before the avalanche is triggered. Characteristic velocity fields during these rearrangements are presented in Sec. V, in particular, the distribution of the velocities and their mean values are analyzed in detail in Secs. V A and V B. In Sec. VI, we present a comparison between the contact network at the beginning of the experiment and just before the avalanche starts. These results are discussed in Sec. VII.

II. EXPERIMENTAL SETUP

The experimental setup is shown in Fig. 1. Wood disks of mass $m=0.76\pm0.03$ g and diameter $d=14.16\pm0.06$ mm are placed inside a transparent acrylic thin cell with a gap of 6.5 mm, slightly larger than the thickness $\phi=6.30\pm0.02$ mm of the disks. The box has a length L

*Electronic address: maaguir@fi.uba.ar
†Electronic address: acalvo@fi.uba.ar
‡Electronic address: iippoli@fi.uba.ar

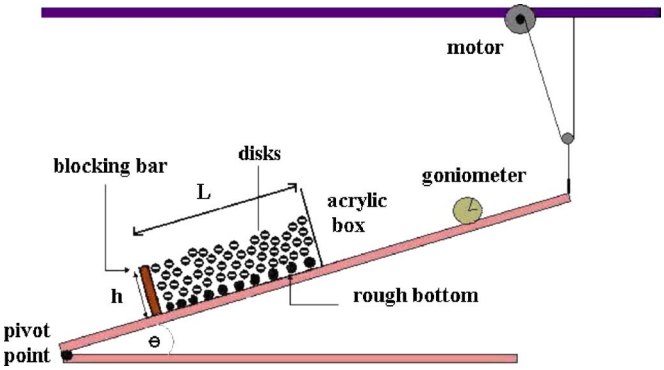

FIG. 1. (Color online) Experimental setup.

=45 cm and a variable height. In order to obtain disordered systems, a rough base of 24 disks is glued to the bottom giving a packing fraction of 0.7. The packing height h was varied by regulating the height of the downstream lateral wall (blocking bar). The coordinate y is equal to 0 at the rough bottom and increases toward the free surface. The axis x is parallel to the rough bottom, the blocking wall is located at $x=0$ and flow is oriented toward negative x values. The cell is mounted over a plane which is slowly tilted, at constant speed $\omega=2.5°/\text{min}$, until an avalanche takes place. A digital camera mounted on one of the sides provides a lateral view of the system, which is tape recorded (25 frames per second) until the avalanche stops. The images are analyzed by digital treatment: for each rearrangement visually detected from the tapes, particles are tracked every $\frac{1}{12}$ s.

In order to track the disks, they are painted in black and a white line is painted across a diameter.

Packings were always constructed with the same procedure in order to obtain a constant initial packing fraction, which has been found to influence the stability of the system [1,9,10]. The coordination number distributions were determined for ten systems in order to verify the disorder of the packings. The mean coordination number is $Z=3.8\pm0.4$, which indicates a stable disordered system [11].

III. AVALANCHE PROCESS

As said in Sec. I the primary objective of these 2D experiments is to analyze the avalanche process and to compare the results with those obtained in 3D sphere packings [1]. The second one is to verify the occurrence of packing rearrangements prior to the avalanche, as observed in 3D experiments, and to study whether those rearrangements involve only superficial grains or the bulk of the packing.

As described in the previous section, the packing is slowly tilted until the avalanche is triggered. An avalanche is said to occur when a considerable number of disks (one layer or more) is displaced out of the cell. Before this catastrophic event occurs, several small and big internal rearrangements are observed. In this section the analysis of the avalanche process is presented and in the next one we describe the experimental observations about previous grain displacements.

The tilt angle of the cell when the avalanche begins is called the maximum angle of stability θ_M (see Fig. 2). When

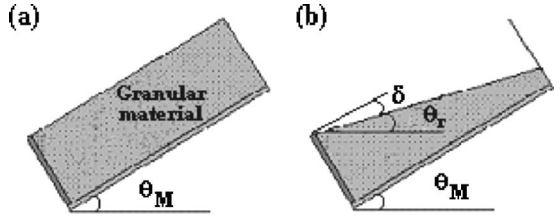

FIG. 2. (a) Maximum angle of stability θ_M, where the avalanche begins. (b) Final configuration for thick packings ($N>7$). White zone (wedge of angle δ) is proportional to the number of disks displaced out of the system.

it ends, the free surface of the packing is no longer parallel to the bottom of the cell but forms an angle δ with it and an angle $\theta_r=\theta_M-\delta$ (angle of repose) with the horizontal (Fig. 2).

The variation of θ_M with the height of the packing has been studied. In Ref. [1] it was shown that, for 3D thick systems, neither θ_M nor θ_r depends on packing height. The same behavior is found in this case as shown in Fig. 3. N is defined as $N=h/d$, where h is the packing height. Systems with different heights were analyzed: $\langle N\rangle=7.4$, 10, and 15.3. These packings have a total number of disks $n_{total}=240$, 360, and 480, respectively. As in three-dimensional experiments [1], it was determined that at least ten identical experiments had to be performed for each value of N. Neither the mean value nor the standard deviation presents measurable variations when more experiments are added. Therefore, 40 experiments were carried out: ten were done for $N\simeq7.4$ and $N\simeq10$, and 20 for the thicker system $N\simeq15.3$ where rearrangements will be studied in detailed (Secs. IV–VI).

The mean values of θ_M and θ_r are plotted in Fig. 3 as a function of N. Taking into account all 40 measurements it can be seen that $\langle\theta_M\rangle=36°\pm3°$ and $\langle\theta_r\rangle=23°\pm4°$ for all studied systems.

Furthermore, as in 3D experiments [1], it is also observed here that for thick systems ($N>7$), only n_{av} superficial disks are involved in the avalanche ($n_{av}\leqslant96$). The rest of the disks remain *almost* motionless: in many cases, it is observed that perturbation (disks moving a distance less than d) can extend throughout the whole packing. It is also verified that the

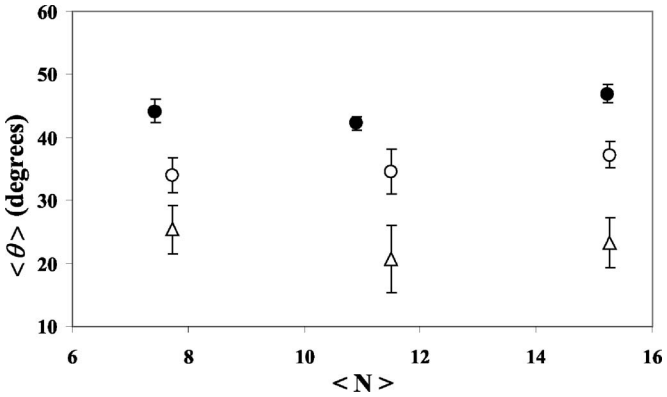

FIG. 3. Maximum angle of stability (○) and angle of repose (△) for disordered systems and maximum angle of stability for ordered systems (●) of different heights ($\langle N\rangle=\langle h\rangle/d$).

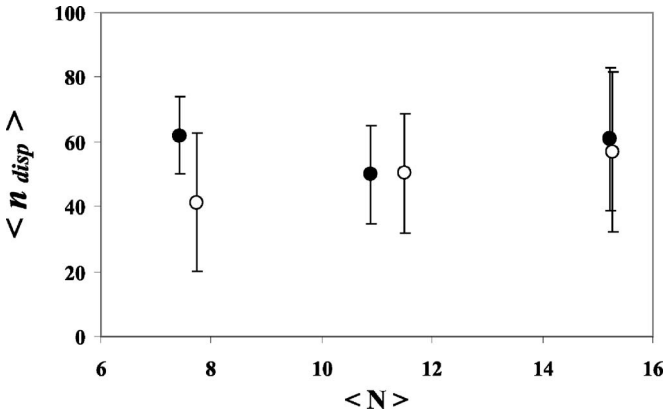

FIG. 4. Mean number of disks displaced out of the system during the avalanche for disordered (○) and ordered (●) packings of different heights ($\langle N\rangle = \langle h\rangle / d$).

number of disks displaced out of the cell during the avalanche is $n_{disp}=n_{av}/2$, independently of the value of N. This result is shown in Fig. 4 where $\langle n_{disp}\rangle$ (mean number of displaced disks) is plotted as a function of N. So the main characteristics of the 2D avalanche process are found to be similar to those observed in the 3D packing.

In order to analyze the influence of the system disorder, several experiments (at least ten) were performed with the disks ordered in a periodic hexagonal network. Ordered systems of different heights were constructed. In this case, the system is clearly layered, containing 31 or 32 disks in each layer.

Small differences between disk diameters ($d = 14.16 \pm 0.06$ mm) can produce differences in the network and introduce disorder in the packings. In order to be sure that the initial condition is the same, we have constructed each packing exactly in the same way: disks were numbered and placed always at the same position and with the same orientation.

Several differences with respect to the disordered systems were observed: (a) no rearrangement of the packing occurs prior to the avalanche; (b) the maximum angle of stability is larger than in the disordered case, $\langle \theta_M\rangle = 44.0° \pm 2.3°$; and (c) the mass displacement during the avalanche is layer by layer and as a consequence $\langle \theta_R\rangle \approx \langle \theta_M\rangle$ (after the avalanche, the free surface remains parallel to the bottom of the cell); nevertheless, a small wedge of disks are stopped near the blocking bar and $n_{disp} \simeq n_{av} - 1$. In Figs. 3 and 4 ordered system results are superimposed with black symbols.

The next step was to study in detail the motion of disks inside the packing before the avalanche occurs.

IV. REARRANGEMENTS: EXPERIMENTAL OBSERVATIONS

As the number of disks taking part in the avalanche does not depend on the height of the packing, the internal reorganization of disks previous to the avalanche was studied in the larger disordered system. So 15 experiments were studied in detail for $N \simeq 15.3$ systems with a total number of disks $n_{total}=480$.

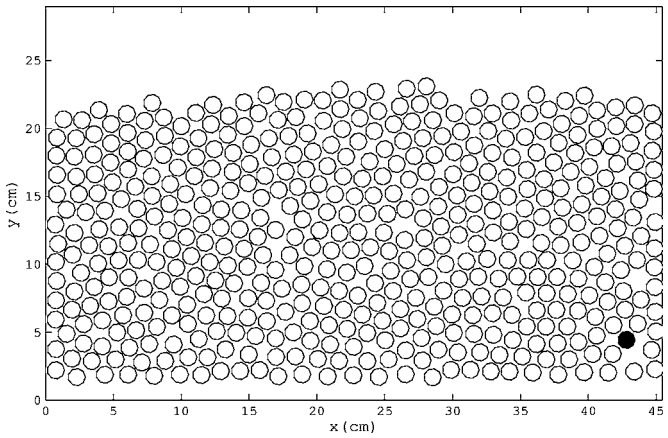

FIG. 5. View of a small event in the bulk: in black the disk that has moved.

The first remarkable experimental observation is that small rearrangements (up to three or four disks involved) of both the surface and the bulk of the packing occur at all times during the experiment. Those taking place at the surface correspond to the fall of one disk which then pushes one or two more. Motions of a few disks in the bulk of the packing are usually due to the rupture of arches or are produced by the slip of a few disks beneath an arch. In Fig. 5 a digitized image of a typical small rearrangement in the bulk is shown: the black disk is the one that has moved.

Large reorganizations of the packing are also observed throughout the experiment though they are more likely to appear for tilt angles of the system larger than 17°. A large rearrangement may involve up to 40% of the disks and a large fraction of the free surface. In Fig. 6 an example is presented. As before, black disks are the ones that have moved during the reorganization of the packing. The number of such collective events observed during an experiment varies between 3 and 7.

An important feature of large events is that almost no mass is displaced out of the cell although in some cases the number of moving disks is twice larger than the ones moving during the avalanche. For that reason we call these collective motions internal rearrangements.

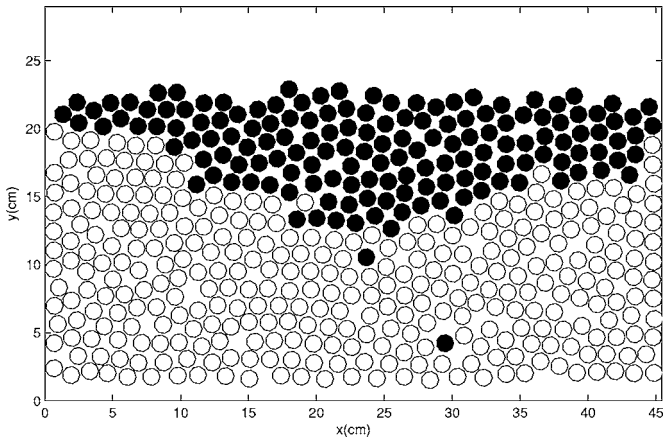

FIG. 6. View of a large event: in black disks that have moved.

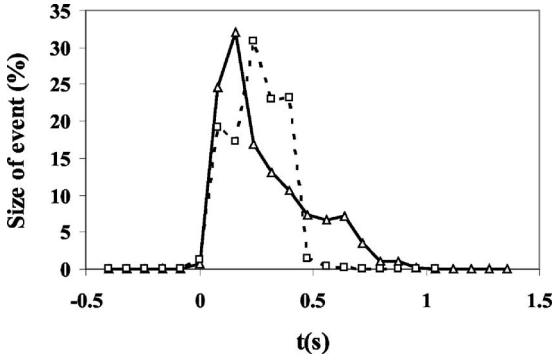

FIG. 7. Evolution of the percentage of disks in motion as a function of time during a rearrangement that stops either slowly (△) or suddenly (□). Rearrangement begins at $t=0$ s.

The development of large rearrangements is always sudden; in less than 0.08 s (one frame) about 100 disks (20% of the total number of disks) may be set in motion. Instead, stopping may be as sudden as the development or much slower. In Fig. 7 the time variation of the percentage of moving disks is displayed for large rearrangements with sudden and slow stops. It can be seen that in both cases the total development of the rearrangement takes less than 0.3 s while the decay lasts for 0.25 s in the quicker event and nearly 0.8 s in the slower one.

Moreover, in some cases, two large rearrangements are produced in cascade: before the motion of disks included in the first one has finished, a second one is triggered. In that case the temporal evolution of the reorganization displays two peaks as shown in Fig. 8.

It is interesting to study in more detail these sudden movements of the packing in order to establish if they influence the start of the avalanche. The next two sections are devoted to the quantitative analysis of the velocity fields of the disks and of changes in the internal structure of the packing produced by their reorganization.

V. VELOCITY FIELDS

From image analysis and particle tracking, velocity fields were obtained for the 50 large events observed in the thickest

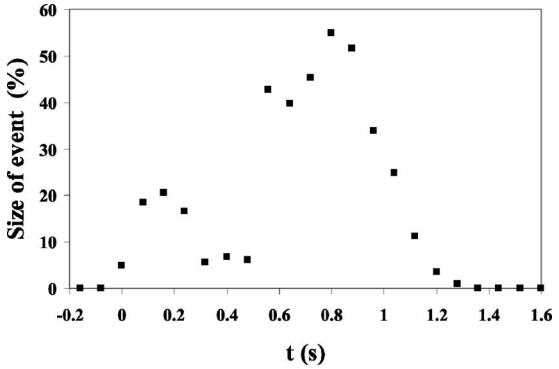

FIG. 8. Evolution of the percentage of disks in motion as a function of time during a rearrangement when two rearrangements occur in cascade. Rearrangement begins at $t=0$ s.

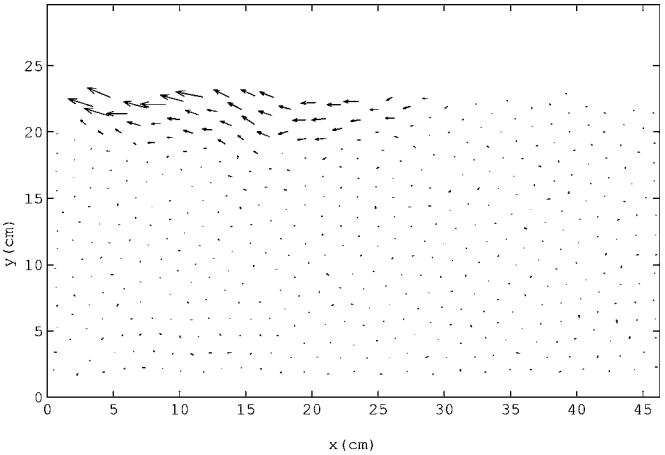

FIG. 9. Velocity field mostly tangential to free surface.

disordered systems. For each rearrangement visually detected from the tapes, particles are tracked every $\frac{1}{12}$ s. About 60% of the trajectories have between three and seven points and 20% have from 20 to 50 points (corresponding to disks in the upper layers which have longer free mean paths). These trajectories assure us that disks do not get trapped—nor oscillate—in the interparticle spacing but they "collectively flow" along a distance larger than one diameter. Only 20% of the trajectories, corresponding to disks in layers near the bottom, have two points and these points are separated by a distance which may be smaller than one diameter. It is neither expected, nor visually observed, that disks in these bottom layers have velocities large enough to collide during the time between both frames, oscillating back and forth due to collisions. However, in these cases we have also analyzed even and odd fields of each frame (time elapsed between them is $\frac{1}{50}$ s) and we have not observed differences from the velocities obtained every $\frac{1}{12}$ s.

Two characteristic velocity fields are shown in Figs. 9 and 10. In some rearrangements, like the one presented in Fig. 9, the flow is mainly tangential to the free surface and flow is guided by faults in the packings. In others (Fig. 10), the rearrangements can affect the deeper layers due to regions of

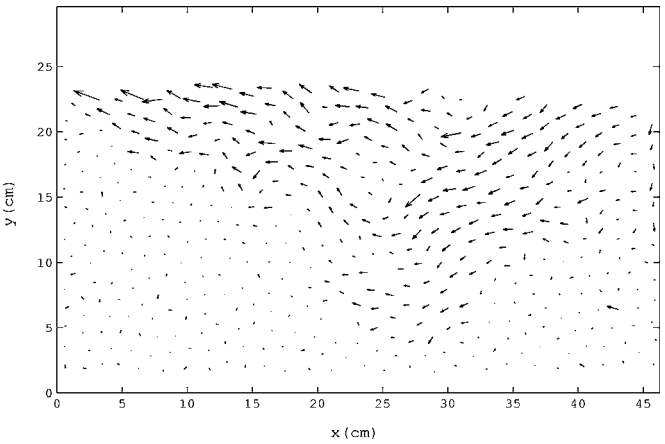

FIG. 10. Velocity field affecting inner layers due to availability of empty space.

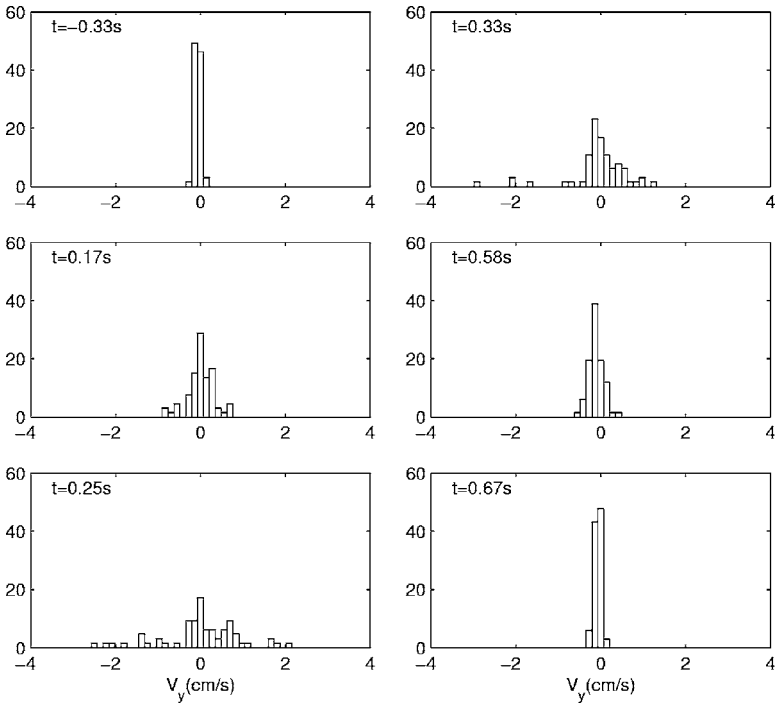

FIG. 11. Characteristic velocity distribution for V_y in slice L_6, at different times during the same event. The system is not moving for $t<0$ and $t\geqslant 0.667$ s.

lower local compacity available to moving disks and triggered by ruptures or slides near arches in the bulk. The latter leads to a flow with a strong component perpendicular to the free surface, extending deeper into the system.

A. Distribution of velocities

Disordered systems were divided into slices of thickness $2d$, labeled L_i with $i=1$ for the rough bottom and $i=8$ for the free surface. For each large rearrangement, disk velocity distributions were obtained in every slice and at all time steps (frames) during the event. Distributions were obtained for velocity components parallel and perpendicular to the free surface ($\hat{x}$ and $\hat{y}$, respectively), and for $|V|=\sqrt{V_x^2+V_y^2}$.

For each event, $t\equiv 0$ s is the time when the rearrangement actually begins, but velocities were also determined 0.4 s before ($t<0$) and 0.4 s after the beginning and end of each event.

Rearrangements can start anywhere in the system and perturbations may extend to all slices. Characteristic distributions of V_y and V_x are shown in Figs. 11 and 12, respectively.

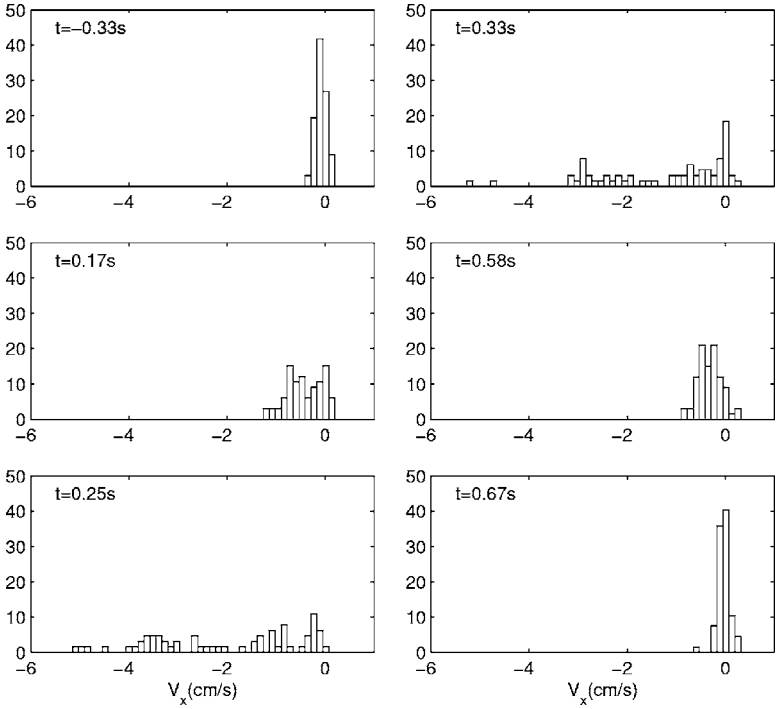

FIG. 12. Characteristic velocity distribution for V_x in slice L_6, at different times during the same event. The system is not moving for $t<0$ and $t\geqslant 0.667$ s.

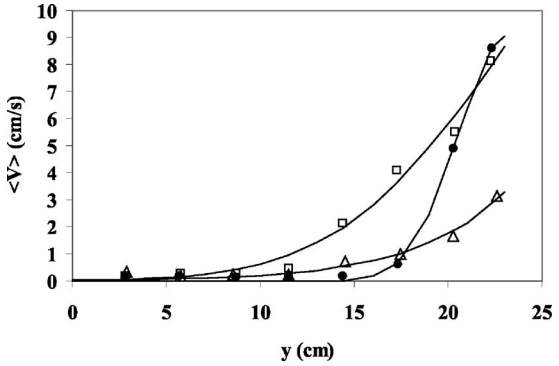

FIG. 13. Mean velocity profiles (exponential △, mixed □, and half Gaussian profiles ●); y is zero at the bottom of packing and maximum at the free surface. Solid lines are the corresponding fittings with $\lambda=3.3d$, $5.6d$ and $\sigma=6d$, $1.8d$, respectively.

The experimental error on the position of the disks is about $0.05d$, or about $0.1d$ on the displacement lengths.

It can be seen that the component V_y (Fig. 11) remains quite symmetrical during the whole process, with a peak of the distribution at $V_y \simeq 0$. At some times ($0.25 \leqslant t \leqslant 0.4$ s) the largest downward velocities ($-\hat{y}$) of the disks are observed as they migrate toward empty spaces below.

Figure 12 shows that all disks move in the $-\hat{x}$ direction: upstream flow does not exist. At a first stage most of the disks stay at rest or move at low velocities ($V_x < 2$ cm/s). At longer times the velocities of the disks in the slice get more widely distributed and reach values larger than 5 cm/s. Finally disks start to stop ($t=0.58$ s) and a Gaussian distribution with a mean value at $V_x=0$ is retrieved ($t=0.67$ s). A similar behavior is observed for $|V|$.

Particular cases are slices L_1 (bottom) and L_8 (surface). The slice L_1 is mostly undisturbed because it is in contact with the fixed rough bottom which constrains the disk motion. On the other hand, disks in slice L_8 are easily set in motion and larger velocities are found in this slice.

B. Velocity profiles

In order to analyze the above described dependence of the velocity on the distance to the rough bottom, mean values $\langle \mathbf{V}_i \rangle$ were computed for each slice at a given time. In this way a mean velocity profile is obtained for every frame of each rearrangement. Mean velocity profiles can be decomposed in two different behaviors: an exponential or half Gaussian increase from the bottom (L_1) to the free surface (L_8), but in most of the cases it is not possible to describe the profile in terms of one behavior or the other: a mixed behavior is observed (Fig. 13). As was said in Sec. I a similar mixed behavior has also been reported [7,8] in a 3D experiment. In general, these behaviors have been already observed separately [4,7] or altogether [12,7,8].

All these previous works deal with a steady state forced by an external constant shear while in our experiments internal disk reorganizations are only due to contact network and gravity effects and, in consequence, they are not stationary. However, the 300 velocity profiles obtained for each temporal step of every large rearrangement produced in all the 15 experiments performed can be well fitted by a combination of an exponential and a Gaussian term:

$$\langle \mathbf{V}(y) \rangle = V_{sup} e^{(y-y_{sup})/\lambda} e^{-(y-y_{sup})^2/2\sigma^2}, \tag{1}$$

where y is the distance to the rough bottom, and V_{sup}, y_{sup}, λ, and σ are fitting parameters. The values of y_{sup} obtained from fitting were in all cases compatible with the actual height of the packing: $y_{sup}=15.3d \pm 0.3d$. As profiles are determined during the full duration of an event, V_{sup} can take values from almost zero up to a maximum of around $8d$ s^{-1}. λ and σ describe the decay lengths of the exponential and Gaussian components, respectively, and the values obtained show that 64% of the profiles are purely exponential (triangles in Fig. 13), only 3% of the profiles are purely Gaussian (black dots in Fig. 13), and 33% are a combination of both contributions (squares in the same figure). Solid lines are the corresponding fittings with $\lambda=3.3d$, $\sigma=1.8d$, $\lambda=5.6d$, and $\sigma=6d$, respectively.

However, more interesting information is achieved by comparing the percentages of both types of velocity profiles obtained during the first large rearrangement of each experiment with the same percentages during the last one, that is, with that occurring just before the avalanche. In fact, considering only the first large internal reorganizations of each experiment one finds that 76% of the profiles correspond to a pure exponential behavior with $\langle \lambda \rangle = 3.2d \pm 0.2d$ and only 24% to a mixed exponential-Gaussian one with $\langle \lambda \rangle = 7.0d \pm 0.5d$ and $\langle \sigma \rangle = 6.2d \pm 0.3d$. And analyzing the last event previous to the avalanche, the percentage of pure exponential profiles decreases to 54% ($\langle \lambda \rangle = 3.0d \pm 0.5d$) while the one of mixed profiles increases to 41% ($\langle \lambda \rangle = 5.2d \pm 0.6d$ and $\langle \sigma \rangle = 4.2d \pm 0.5d$), and 5% of pure half Gaussian profiles appears ($\langle \sigma \rangle = 1.6d \pm 0.3d$).

VI. ANGULAR REARRANGEMENT OF DISK NEAREST NEIGHBORS

An important feature of a two-dimensional packing is the contact network, i.e., the location of the nearest neighbors around each grain. Its knowledge provides a way to estimate the disorder of the system. In fact, different order parameters, translational and orientational, have been suggested in the literature and it is still an open matter which is the best candidate for a given granular system (e.g., packing fraction or density, bond orientations, and local Q_6 order metric). Bond orientations (or angle distribution of neighbors) and other orientational parameters have been used as good order parameters [3,11,14].

Therefore, the study of how the contact network changes when large rearrangements take place might be a useful tool to clarify the role played by these rearrangements in the development of the avalanche.

In order to describe the initial contact network of the packing, the angles α_i between successive neighbors of each disk were measured at the beginning of each experiment (see Fig. 14). As not all events affect the packing deepest layers we only determine contacts in superficial layers above 70%

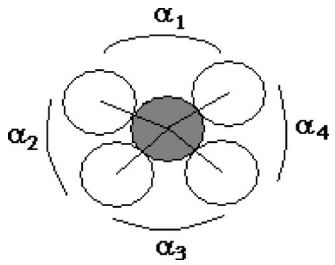

FIG. 14. Angles between nearest neighbors of a disk.

of the total height of the packing, in order to avoid an excessive influence on the results of the motionless disks.

Histograms for the measured angles α are obtained for data separated into 36 bins centered every 10° (0°, 10°, 20°,…,350°). For example, the second bin, centered at 70°, takes into account angles between 65° and 75°.

The angle α may only vary between 60° and 300° and periodic networks lead to a single value of α for all disks in the bulk of the packing (α=60° for a hexagonal network, for example). In this way, the broadest the distribution of α values, the more disordered the system.

In Fig. 15 (dashed line) the distribution of α (as a percentage) is shown for the initial state of the hexagonal ordered packing. It can be seen that 80% of the angles between neighbors are equal to 60°. In the same figure, data corresponding to the initial state of the 15 disordered packings studied are superimposed with a solid line. It is clear that in our systems around 60% of the contacts do not correspond to an ordered network.

In each disordered system, angles α_i are measured again just before the avalanche begins, that is, after all the large rearrangements have occurred. The difference between this final distribution and the initial one is displayed in Fig. 16. A decrease of the peak at α=60° and an increase of the distribution for larger angles are observed. That is, in mean value successive internal reorganizations in the packing increase its disorder until the avalanche takes place.

This result, together with observations presented in Sec. III, that in completely ordered packings, where no internal

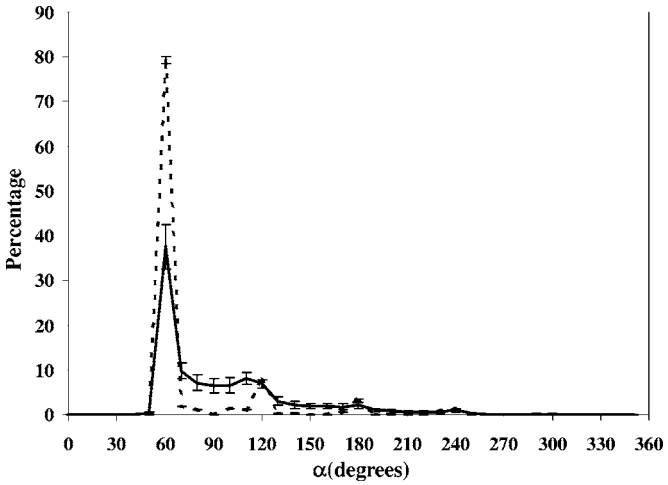

FIG. 15. Initial distribution of α, angles between neighbors of a disk, in superficial layers for an ordered hexagonal system (dashed line) and a disordered system (solid line).

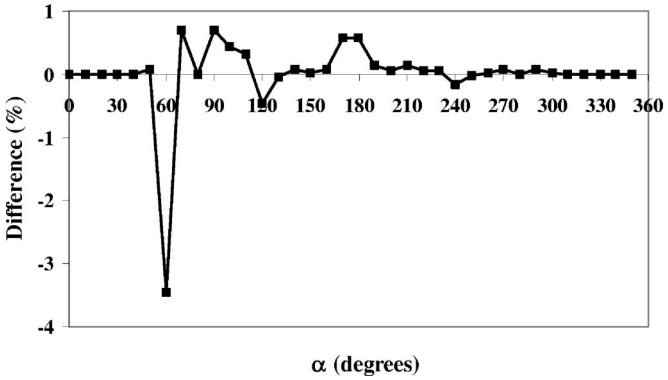

FIG. 16. Difference between final and initial distributions of α, angles between neighbors of a disk, for disordered systems.

reorganizations are possible due to the lack of free space, the avalanche only takes place at a larger inclination angle of the cell, seems to indicate the existence of a correlation between the degree of disorder in the system and the angle at which it loses its stability.

The above statement is verified by defining the fraction of neighbors separated at α=60° as the order parameter of the system (OP) and plotting the angle at which the avalanche takes place versus the OP. In Fig. 17 the variation of θ_M with the OP is plotted for the 15 experiments performed in the thickest disordered systems. Notice that the point at $\langle N \rangle$ =15.3 in Fig. 3 is the mean value of open squares in Fig. 17. That is, under similar initial conditions the avalanche occurs at different angles $\theta_M(33° < \theta_M < 41°)$ and Fig. 17 shows that the system loses its stability at higher angles as the order parameter of the packing just before the avalanche, increases. As previously said, ordered hexagonal systems lose their stability at much higher angles (see Fig. 3). The point corresponding to an ordered system of the same height is superimposed in Fig. 17 (black square) only to show that data in a wide range of the OP display an increasing tendency. In this way, the idea that the greater the packing order, the higher the angle at which the avalanche occurs, is reinforced.

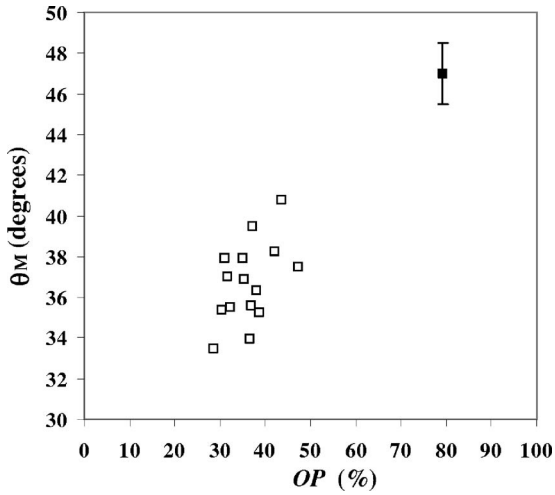

FIG. 17. Maximum angle of stability as a function of the system order parameter for disordered (□) and ordered (■) packings of the same height.

VII. DISCUSSION AND CONCLUSIONS

It was shown that the main features of avalanches in 3D granular packings can also be observed in 2D systems. In disordered systems, small and large rearrangements (without mass displaced out of the system) occur prior to the avalanche both in the surface and in the bulk. No rearrangements (of any size) were observed in hexagonal ordered systems. The avalanche is triggered when θ_M is reached and 20 disks or more are displaced out of the box. For disordered thick systems ($N>7$), in which characteristic angles do not change as the system increases its height, the surface of the packing after the avalanche is plane and the angle of repose θ_r is defined and neither the avalanche mass nor the characteristic angles depend on the system height. The packing stability threshold θ_M is bigger in ordered packings and after the avalanche the free surface remains parallel to the bottom of the cell ($\langle\theta_R\rangle \approx \langle\theta_M\rangle$).

Velocity profiles of large reorganizations occurring in disordered systems were well described by a combination of an exponential and Gaussian behavior. This result shows that previous association of the first dependence to two-dimensional systems and the latter to 3D ones [13] is not valid in the geometrical conditions used in this work.

Furthermore, it was found that considering only the first large event most of the profiles (74%) are well described by purely exponential dependence. On the other hand, analyzing the last event previous to the avalanche, that percentage decreases while the number of combined profiles increases and, even more, 5% of pure Gaussian behavior is found. In previous work [7] it was shown that the exponential contribution is related to layering displacement (which occurs in ordered systems) and the Gaussian part to disorder.

In addition, the study of changes in the internal structure of the packing, presented in Sec. VI, shows that successive reorganizations previous to the avalanche increase the system disorder.

In conclusion, the experimental results in disordered systems (velocity profiles and changes in the internal structure) together with the fact that ordered packings have a value of the maximum angle of stability larger than disordered ones, confirm that one of the main effects of rearrangements is to increase the disorder of the system. Moreover, as the disorder of the system increases its stability threshold decreases.

ACKNOWLEDGMENTS

We thank J. P. Hulin and E. Clément for invaluable suggestions for this work and M. F. Trunkhardt and G. Mayama for important contributions. This work was supported by the programs I 027 (SECyT UBA) and PICT No. 12-8849 (ANCyT).

[1] M. A. Aguirre, N. Nerone, A. Calvo, I. Ippolito, and D. Bideau, Phys. Rev. E **62**, 738 (2000).
[2] N. Nerone, M. A. Aguirre, A. Calvo, D. Bideau, and I. Ippolito, Phys. Rev. E **67**, 011302 (2003).
[3] L. Staron, Ph.D. thesis, Institut de Physique du Globe de Paris, 2002 (unpublished), Chap. III, pp. 68–70.
[4] T. S. Komatsu, S. Inagaki, N. Nakagawa, and S. Nasuno, Phys. Rev. Lett. **86**, 1757 (2001).
[5] D. Bonamy, F. Daviaud, L. Laurent, M. Bonetti, and J. P. Bouchaud, Phys. Rev. Lett. **89**, 034301 (2002).
[6] C. T. Veje, D. W. Howell, and R. P. Behringer, Phys. Rev. E **59**, 739 (1999).
[7] D. M. Mueth, G. F. Debregeas, G. S. Karczman, P. J. Eng, S. R. Nagel, and H. M. Jaeger, Nature (London) **406**, 385 (2000).
[8] D. M. Mueth, Phys. Rev. E **67**, 011304 (2003).
[9] P. Evesque, D. Fargeix, P. Habib, M. P. Luong, and P. Porion, Phys. Rev. E **47**, 2326 (1993).
[10] S. R. Nagel, Rev. Mod. Phys. **64**, 321 (1992).
[11] D. Bideau, A. Gervois, L. Oger, and J. P. Troadec, J. Phys. (France) **47**, 1697 (1986).
[12] C. Josserand, Europhys. Lett. **48**, 36 (1999).
[13] G. Debregeas and C. Josserand, Europhys. Lett. **52**, 137 (2000).
[14] A. Donev, S. Torquato, F. H. Stillinger, and R. Connelly, J. Appl. Phys. **95**, 989 (2004).